Sains Malaysiana 49(11)(2020): 2801-2809
http://dx.doi.org/10.17576/jsm-2020-4911-19

Photophysical Properties and Energy Transfer Mechanism in PFO/TiO_2/MEH-PPV Nanocomposite Thin Films

(Sifat Fotofizikal dan Mekanisma Pemindahan Tenaga dalam Filem Nipis Nano Komposit PFO/TiO_2/MEH-PPV)

SAMEER ALBATI, MOHAMMAD HAFIZUDDIN HJ. JUMALI*, BANDAR ALI AL-ASBAHI, SAIF M.H. QAID & CHI CHIN YAP

ABSTRACT

Improvement in photophysical properties of poly-9,9-dioctylfluorene (PFO)/10 wt. % TiO_2 nanoparticle thin film as a result of systematic additions of poly(2-methoxy-5(2-ethylhexyl)-1,4-phenylenevinylene (MEH-PPV) were investigated. The nanocomposite blends were prepared with additions of MEH-PPV up to 3.0 wt. % of the total weight. All blends were prepared using the solution blending method and subsequently spin-coated onto glass substrates. The UV-Vis absorption and photoluminescence characterizations showed the intensification of the primary-color emissions of the thin films with the Förster resonance as the primary energy transfer mechanism from PFO to MEH-PPV. Important photophysical parameters, such as the Förster radius (R_o) excited state lifetime (τ), fluorescence quantum yield of the donor (φ), quenching constant (k_{sv}), quenching rate constant (k_q), distance between the donor and acceptor (R), energy transfer lifetime (τ_{ET}), and energy transfer rate (k_{ET}) display better values with increasing the contents of MEH-PPV by 2.5 wt. %, suggesting an ordered improvement on the photophysical properties of the thin film. Finally, a possible underlying mechanism describing the enhancement of the photophysical properties was proposed.

Keywords: Donor/acceptor; energy transfer properties; Förster resonance energy transfer; optical properties

ABSTRAK

Peningkatan sifat fotofizikal filem nipis adunan poli-9,9-dioktilflorin (PFO)/10 bt. % nanozarah TiO_2 dengan penambahan secara sistematik poli(2-metoksi-5(2-etilheksil)-1,4-fenileenevinilene (MEH-PPV) adalah dibuktikan. Adunan nanokomposit ini disediakan dengan menambah MEH-PPV sehingga 3.0 bt. % daripada berat keseluruhan. Kesemua adunan disediakan menggunakan teknik adunan larutan dan kemudiannya dimendapkan ke atas substrat kaca menggunakan teknik salutan berputar. Pencirian penyerapan UV-Vis dan fotoluminesens menunjukkan peningkatan keamatan pancaran filem nipis dengan pemindahan tenaga resonans Förster sebagai mekanisma pemindahan tenaga primer daripada PFO kepada MEH-PPV. Semua parameter fotofizikal yang penting seperti jejari Förster (R_o), jangka hayat keadaan teruja (τ), hasilan kuantum pendarfluor oleh perderma (φ), pemalar pelindapkejutan (k_{sv}), pemalar kadar pelindapkejutan (k_q), jarak antara penderma dan penerima (R), jangka hayat pemindahan tenaga (τ_{ET}) dan kadar pemindahan tenaga (k_{ET}) menunjukkan nilai yang lebih baik dengan penambahan MEH-PPV sekaligus membuktikan penambahbaikan yang teratur terhadap sifat fotofizikal filem nipis. Dengan kehadiran nanozarah, keamatan sinaran warna primer telah meningkat dengan pancaran yang seimbang antara PFO dan MEH-PPV berjaya dicapai pada kandungan MEH-PPV sebanyak 2.5 bt. %, mencadangkan peningkatan yang teratur pada sifat fotofizik filem nipis. Kesimpulannya, mekanisma yang sesuai untuk menerangkan peningkatan sifat fotofizikal turut dicadangkan.

Kata kunci: Pemindahan tenaga resonan Förster; penderma/penerima; sifat optik; sifat pemindahan tenaga

INTRODUCTION

Despite great advancement in display technologies, fabrication of excellent white organic light-emitting diodes (WOLEDs) continues to attract the attention of researchers worldwide. Generally, WOLEDs can be obtained from diode emission of various wavelengths in the visible region of the electromagnetic (EM) spectrum. However, it is very challenging to produce this type of diode, particularly when using single active material. An alternative approach is the combination of primary lights produced by selective polymer-polymer blends (Lee et al. 2019; Zhang et al. 2017; Zhou et al. 2018). One of the combinations with the most potential is a blend of poly-9,9-dioctylfluorene (PFO) and

poly(2-methoxy-5 (2-ethylhexyl)-1,4-phenylenevinylene (MEH-PPV) (Cossiello et al. 2010; Madhwal et al. 2010; Prakash & Katiyar 2016). In this blend, PFO with highest occupied molecular orbital (HOMO) and lowest unoccupied molecular orbital (LUMO) energies of -5.8 and -2.6 eV, respectively, acts as a donor, while MEH-PPV (HOMO of -5.3 and LUMO of -2.8 eV) (Shin et al. 2009) acts as an acceptor. The energy transfer mechanism between these polymers has been confirmed to be Förster resonance energy transfer (FRET) (Cossiello et al. 2010).

Initial work on this blend focused on achieving efficient energy transfer (Liu et al. 2001). Since then, the successful fabrication of WOLEDs using this polymer combination has been reported (Huang et al. 2006; Kasparek & Blom 2017; Shen et al. 2006; Shin et al. 2009). However, optophysical issues, such as limited brightness and luminance efficiency, continue to be the major challenges related to PFO/MEH-PPV-based WOLEDs. To overcome these challenges, several approaches have been proposed such as the fabrication of multilayered polymers (Yan et al. 2015), introduction of an electron-injection and a hole-blocking layer (Yang & Zhuang 2011), as well as the addition of conducting and semiconducting nanoparticles (Al-Asbahi 2018).

The WOLEDs based on the PFO/MEH-PPV blend can only be fabricated under two conditions, that is, if incomplete energy transfer occurs and both polymers have the same emission intensity to cover the whole visible spectrum (Shen et al. 2006). To achieve these conditions, the maximum ratio of MEH-PPV in the blend was limited to 1 wt. % (Shin et al. 2009). Researchers have argued that the luminance efficiency of OLEDs can be improved by increasing the acceptor ratio (Al-Asbahi et al. 2013a; Su et al. 2005). Unfortunately, an earlier study showed that a high acceptor concentration is not favored due to the formation of dark quenchers (Thomas et al. 2014). Moreover, the addition of more acceptor only causes a dramatic reduction in the PFO emission intensity without meaningful increment in the MEH-PPV emission intensity itself (Huang et al. 2006). As a result, low-efficiency OLEDs with yellowish emission are produced. Complete quenching of the PFO emission was reported at a ratio of 4 wt. % and above (Liu et al. 2001).

The best strategy to enable the addition of more acceptor to the blend is to increase the emission intensity of the donor. Earlier studies on PFO/TiO_2 nanocomposite OLEDs showed that this strategy is possible (Al-Asbahi 2016; Al-Asbahi et al. 2017; Huang et al. 2018). It has been proven that the addition of 10 wt. % of TiO_2 nanoparticles (NPs) remarkably enhances the brightness and efficiency of PFO-based OLEDs through a mechanism known as the charge trapping effect (Jumali et al. 2012). Interestingly, in a subsequent study, the addition of 10 wt. % of TiO_2 NPs to a thin film of the PFO/F7GA blend not only inhibited the formation of dark quenchers but also led to an improved OLED performance (Al-Asbahi 2017). Furthermore, the high values of important FRET parameters support the argument that the energy transfer is more efficient in the presence of TiO_2 NPs.

In this study, the strategy used to enhance the photoluminescence (PL) efficiency of thin films of white PFO/MEH-PPV polymer blends were to increase the emission of the donor. Based on earlier work (Al-Asbahi 2017), all blends were prepared using a constant TiO_2 NP concentration (10 wt. % PFO) while systematically increasing the MEH-PPV concentration (up to 3.0 wt. % PFO). The aim of this work was to increase the limited ratio of the acceptor (MEH-PPV) in PFO/MEH-PPV blends as potential material for WOLEDs. In addition, the energy transfer properties of PFO/MEH-PPV/TiO_2 nanocomposite blends are investigated in more detail in this work. Finally, a suitable mechanism to describe the results is proposed.

Material and Methods

Raw materials used in this work which were PFO (Mw = 58200), MEH-PPV (Mw = 51000), and TiO_2 NPs (P25 Degussa) were purchased from Sigma Aldrich while toluene was bought from Fluka. The solutions were prepared using the solution blending method. Initially, PFO was dissolved in toluene and stirred at 700 rpm for 2 h to produce a solution with fixed concentration of 15 mg mL^{-1}. Subsequently, 10 wt. % of TiO_2 NPs of the total weight was added into the PFO solution before MEH-PPV with different amounts (ranging from 0.5 to 3.0 wt. % of the total weight) were added into the solution to form nanocomposite blends. Then, the blends were constantly stirred at 700 rpm for overnight and finally sonicated for 1 h to obtain homogeneous solutions.

In the present work, the spin coating technique was used to deposit the blends onto 2.4 cm^2 glass substrate to form thin films. The spinning rate was fixed at 2000 rpm for 30 s while each deposition used 80 µL of the prepared blends. To ensure the elimination of the solvent from the films, the thin film samples was heated on a hot plate at 90 °C for 15 min.

The optical absorption and emission characteristics of the thin film samples were determined using a Perkin Elmer Lambda 950 UV–Vis–NIR spectrometer and Edinburgh Instruments FLS920 photoluminescence spectrometer with an excitation wavelength of 370 nm, respectively. In addition, the Dektak 150 Surface Profiler was used to measure the thickness of the films.

Results and Discussion

Figure 1 shows the UV–Vis absorption spectra of pristine PFO thin film, PFO/TiO_2 nanocomposite thin film, and

pristine MEH-PPV thin film. The maximum absorptions of the PFO and PFO/TiO_2 films are observed at 383 nm and that of MEH-PPV film is observed at 504 nm. The high similarity of the absorption spectra of PFO film and PFO/TiO_2 nanocomposite film suggests an insignificant absorption from TiO_2 NPs with large energy band gaps and an insignificant variation of the structure of the polymer. Jumali et al. (2012) reported the same characteristic. The presence of a small peak at 435 nm is attributed to the presence of β-phase chain segments in PFO (Li et al. 2017; Perevedentsev et al. 2016; Winokur et al. 2003). Despite earlier work claimed the presence of β-phase chain segments has some effect on the final optical properties of PFO, observations in the current work indicated no significant impact on the general photon absorption profile of the studied system. With fixed concentration of PFO dissolved in the same type of solvent, the presence of this small peak continues to be observed in all absorption spectra indicating no chemical reaction between the raw materials.

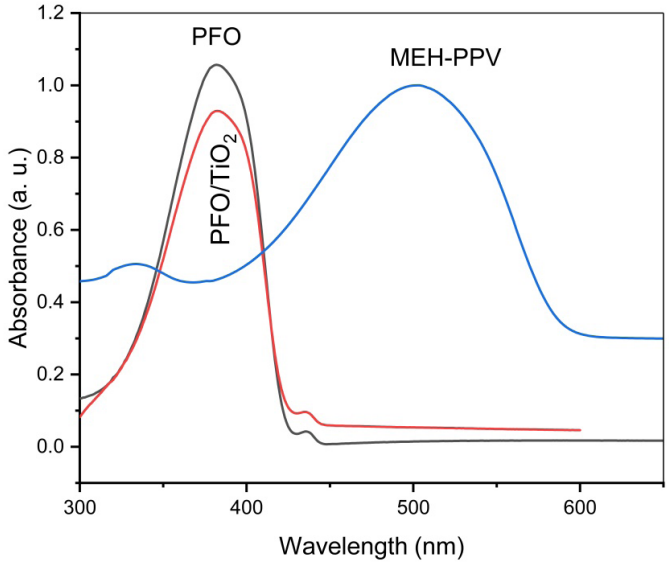

FIGURE 1. Absorption spectra of pristine PFO, PFO/TiO2 and pristine MEH-PPV

The absorption spectra of all blended thin films, with average thickness varies between 116 and 125 nm are shown in Figure 2. All thin films exhibited broad, intense absorption peak between 325 and 425 nm. In addition, weak absorption peak can also be seen at wavelengths between 450 and 575 nm (Figure 2 inset). The former peak is the typical absorption peak of PFO while the latter belongs to MEH-PPV. However, both absorption peaks did not exhibit any systematic enhancement in intensity. This behavior could stem from among others the nonlinear variations in the thickness of film. It is important to note the absence of any new absorption peak in the films suggesting insignificant chemical interaction particularly between the polymers (Jumali et al. 2012). Moreover, the presence of MEH-PPV has negligible effect on general absorption profile of the spectra, hence the wavelength with the maximum absorption for all thin films remain at the same value. Consequently, detailed analysis using Tauc's equation (Hegde et al. 2019) showed that both the direct and indirect energy band gaps (E_{gd} and E_{gi}, respectively) are essentially unchanged after the addition of MEH-PPV (Table 1). These findings are a clear manifestation of the insignificant modification of the electronic structure of the blended materials.

Unlike the band gaps, the band structure disorder estimated from the Urbach energy band tail width (ΔE) (Hegde et al. 2019) displays a strong linear dependency on the MEP-PPV contents (Table 1). The steady increment in the ΔE values is commonly associated with the creation of many localized states within or near the conduction

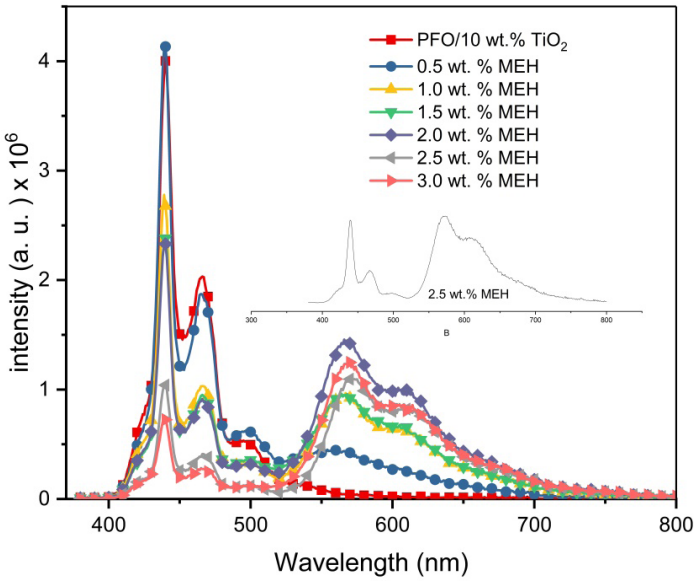

FIGURE 2. Absorption spectra of PFO/10wt.%TiO_2/MEH-PPV (0-3.0) wt.%

band level (Jumali et al. 2012). Consequently, band-to-tail and tail-to-tail electronic transitions are highly probable (Jumali et al. 2012).

Dominant non-radiative Förster-type energy transfer in the blended films is indicated by the huge spectral overlap between the PL spectrum of PFO/TiO_2 and the absorption spectrum of MEH-PPV (Figure 3). This argument is strongly supported by another critical element of Förster-type energy transfer, that is, the Förster radius, R_o, which can be expressed as (1) (Karthikeyan 2017):

$$R_o^6 = \frac{900(\ln 10)\beta^2\varphi_o}{128\pi^5 n^4 N_o} \int F_D(\lambda)\varepsilon_A(\lambda)\lambda^4 d\lambda = \frac{900(\ln 10)\beta^2\varphi_o}{128\pi^5 n^4 N_o} J(\lambda), \quad (1)$$

where n is the refractive index of toluene; N_o is the Avogadro number; β^2 is the orientation factor; φ_o is the fluorescence quantum yield of pristine PFO; λ is the wavelength of the emitted photon; $\varepsilon_A(\lambda)$ is the molar decadic extinction coefficient of the acceptor; and $F_D(\lambda)$ is the normalized spectral distribution of the donor ($\int F_D(\lambda)d\lambda = 1$). The values for n, β^2, and φ_o used in this work are 1.496, 2/3, and 0.72, respectively (Al-Asbahi et al. 2013a).

TABLE 1. The thickness and optical energy properties of PFO/10 wt. % TiO_2 with addition of MEH-PPV

MEH-PPV (wt. %)	Thickness ± 1(nm)	E_{gd} (eV)	E_{gi} (eV)	ΔE (eV)
0	117	2.98	2.846	0.078
0.5	116	2.98	2.846	0.082
1.0	120	2.98	2.846	0.084
1.5	118	2.98	2.846	0.091
2.0	123	2.98	2.846	0.092
2.5	122	2.98	2.832	0.093
3.0	125	2.98	2.825	0.101

Minor variations in the calculated values of Table 2 demonstrate that the concentration of MEH-PPV in the PFO/TiO_2 blends has an insignificant influence on the Förster radius. For effective Försw9iter-type energy transfer, the Förster radius must range between 10 and 100Å(Schweitzer & Schmidt 2003). Interestingly, all values for the calculated R_o are between 50 and 60 Å, thus confirming the Förster-type energy transfer as the primary mechanism in PFO/MEH-PPV/TiO_2 blends. In addition, the systematic reduction in the excited state lifetime (τ) and fluorescence quantum yield of the donor (φ) as a function of the MEH-PPV content demonstrate the improvement in the efficiency of the Förster energy transfer in the studied films (Pandey et al. 1988).

TABLE 2. Förster radius, quantum yield, and lifetime of PFO/10 wt. % TiO_2/MEH-PPV

MEH-PPV content (wt. %)	$R_o(\dot{A})$	φ	$\tau(ps)$
0.5	55.8	0.680	326
1.0	53.4	0.479	230
1.5	53.1	0.417	200
2.0	53.4	0.258	124
2.5	58.9	0.186	89
3.0	52.2	0.124	60

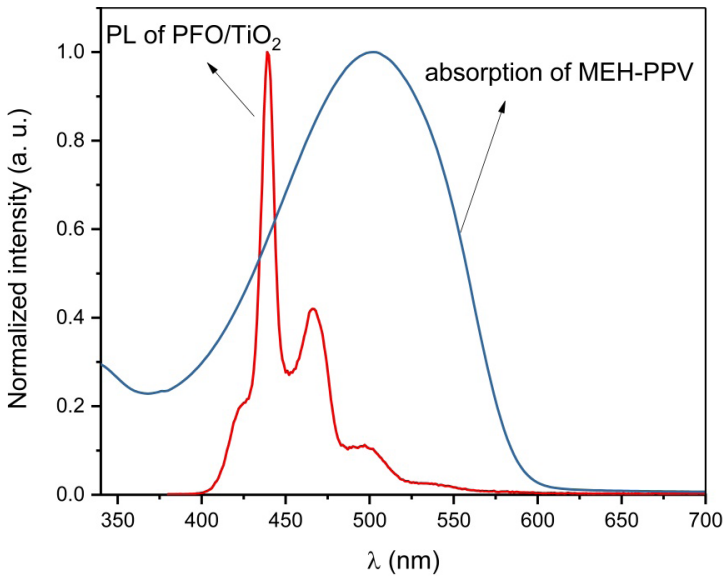

FIGURE 3. Overlap between the absorption spectrum of MEH-PPV and the emission spectrum of PFO/10 wt. % TiO_2

Figure 4 shows the photoluminescence spectra of all PFO/TiO_2/MEH-PPV-blended films. The efficiency of MEH-PPV as acceptor was demonstrated by orderly declining intensities of the PFO peaks. As a result, the emission intensity of MEH-PPV gradually increases before exhibiting a downward trend when its content exceeds 2.0 wt. %.

Based on Figure 4, additional evidence of the efficient energy transfer, that is, the Stern–Volmer constant (quenching constant; k_{sv}) and quenching rate constant (k_q), can be extracted using the following relations (2) and (3) (Ciotta et al. 2019):

$$\frac{I_o}{I} = 1 + k_{SV}[A] \quad (2)$$

$$k_q = \frac{k_{SV}}{\tau_o} \quad (3)$$

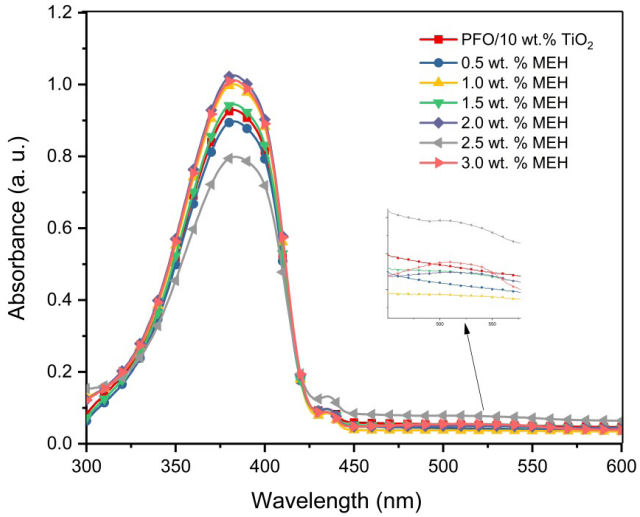

FIGURE 4. Fluorescence spectra of PFO/10 wt. %TiO_2/MEH-PPV (0.0-3.0) wt. %. Excitation at 380 nm

where I_o and I are the fluorescence intensities in the absence and presence of an acceptor, respectively, and [A] is the acceptor concentration. The excited state lifetime of the pristine donor (τ_o) is fixed at 346 ps (Al-Asbahi et al. 2013b). The linear Stern-Volmer plot for the blends is presented in Figure 5. The k_{sv} value obtained from the gradient of the line implies that 2.07 µM MEH-PPV are required to halve the fluorescence of PFO. On the other hand, the value calculated for k_q is 1.40×10^{15} $M^{-1}s^{-1}$, that is, five orders of magnitude higher than the minimum value for efficient energy transfer (Albrecht 2008).

Other important parameters related to the energy transfer, such as the energy transfer lifetime, τ_{ET}, and energy transfer rate, k_{ET}, have been calculated using the following (4) and (5) (Albrecht 2008):

$$\tau_{ET} = \frac{1}{[A]k_q} \tag{4}$$

$$k_{ET} = \frac{1}{\tau_o}\left(\frac{R_o}{R}\right)^6 \tag{5}$$

where [A] is the molar concentration of the acceptor in the blend. In addition, the distance between the donor and acceptor, R, was estimated using (6) (Albrecht 2008):

$$\delta = \frac{R_0^6}{R^6 + R_0^6}, \tag{6}$$

where δ is the energy transfer efficiency, which equals $(1 - I / I_o)$ (Albrecht 2008).

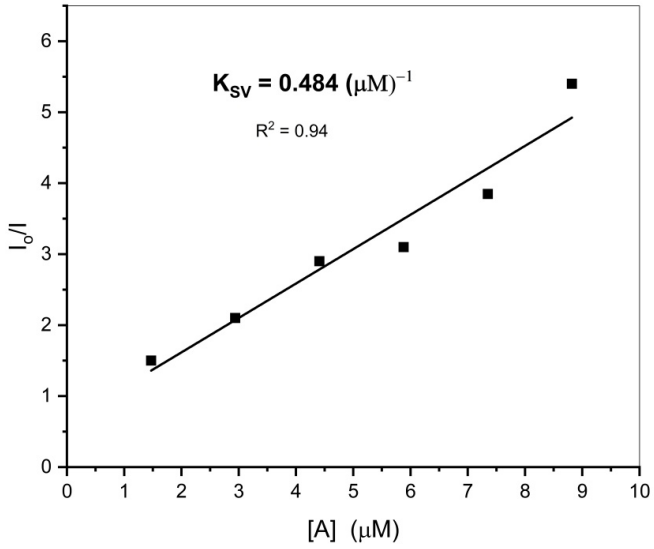

FIGURE 5. Stern-Volmer plot for fluorescence quenching of PFO/TiO_2 by MEH-PPV

All calculated values are presented in Table 3. Except for 0.5 wt. % MEH-PPV, all other values for *R* are in the range of the Förster radius. More importantly, the distance between the donor and acceptor systematically decreases as more MEH-PPV is added to the blend. Remarkably, the τ_{ET} also decreased with the MEH-PPV content, while k_{ET} positively enhances as the distance between donor and acceptor shortens. Interestingly, all trends of these parameters support the above-mentioned findings about the excited state lifetime (τ) and fluorescence quantum yield (φ), confirming the highly efficient energy transfer in current blend films (Albrecht 2008).

To produce white OLEDs, it is desirable that the emitting materials produce photons covering the whole visible region of the EM spectrum. Alternatively, the materials should produce a suitable combination of primary colors with balanced intensities (Shen et al. 2006). A precise ratio between the emitting materials is crucial to achieve a balanced intensity.

TABLE 3. Critical energy transfer distance, energy transfer rate and energy transfer lifetime

MEH-PPV content (wt. %)	$R_o(\AA)$	$k_{ET}(ns)^{-1}$	$\tau_{ET}(ps)$
0.5	89.2	0.2	374
1.0	59.9	1.4	187
1.5	52.4	3.1	125
2.0	48.5	5.2	93
2.5	49.4	8.3	75
3.0	40.2	13.9	62

Balanced emission intensities were successfully achieved at an acceptor concentration of 2.5 wt. % (Figure 4). This value is 2.5 times greater than earlier reported data, signifying the importance of the TiO_2 NPs in the blends (Shin et al. 2009). It is notable that more acceptor can be added to the blends because of the presence of NPs, which is desirable for a more efficient energy transfer. Earlier studies successfully proved that the addition of TiO_2 to PFO enhances the emission intensity through the charge trapping effect (Al-Asbahi et al. 2013b; Jumali et al. 2012). This is possible because TiO_2 has a stronger electron affinity as well as an energy band diagram that is compatible with the polymer. Hence, more excitons are created in the PFO, which in turn allows intense emission during electron–hole recombination. Consequently, more acceptors can be added to the blends.

Because the Förster energy transfer efficiency improves with the addition of MEH-PPV, more acceptor molecules can be excited, which leads to intense emission. Above a concentration of 2.0 wt. %, the emission intensity of MEH-PPV starts to drop. However, this reduction does not imply that the energy transfer from the donor to the acceptor slows down. In fact, the efficient energy transfer from the PFO continues, as manifested by the detection of lower emission. However, instead of fluorescence, the energy received by the MEH-PPV is converted to heat via the formation of dark quenchers (Nedumpara et al. 2008). This observation indicates the preferential energy loss via heat. A similar observation has been reported for PFO/TiO_2/F7GA blend film (Al-Asbahi 2017).

Conclusion

In conclusion, the influence of different MEH-PPV concentrations on the photophysical properties of PFO/10 wt. % TiO_2/MEH-PPV nanocomposite thin films have been investigated. The decrease in the donor emission intensity, increase in the acceptor emission intensity, and high R_o and k_{sv} values with increasing MEH-PPV content are the major indicators for efficient Förster resonance energy transfer in the blend. In addition, all τ, φ, k_q, R, τ_{ET}, and k_{ET} calculations indicate an improvement in the emission efficiency. Because of the charge trapping effect provided by the TiO_2 NPs, more acceptor molecules can be added to the blend to improve energy transfer efficiency and to achieve balanced emissions, which are the two prerequisites for high-efficiency WOLEDs.

Acknowledgments

This work was supported by Universiti Kebangsaan Malaysia grant number DIP-2016-027 and the Deanship of Scientific Research at King Saudi University through Research Group no RG-1440-037.

REFERENCES

Al-Asbahi, B.A. 2018. Influence of SiO_2/TiO_2 nanocomposite on the optoelectronic properties of PFO/MEH-PPV-based OLED devices. *Polymers* 10(7): 800-806.

Al-Asbahi, B.A. 2017. Energy transfer mechanism and optoelectronic properties of (PFO/ TiO_2)/Fluorol 7GA nanocomposite thin films. *Optical Materials* 72: 644-649.

Al-Asbahi, B.A., Haji Jumali, M.H. & AlSalhi, M.S. 2016. Enhanced optoelectronic properties of PFO/Fluorol 7GA hybrid light emitting diodes via additions of TiO_2 nanoparticles. *Polymers* 8(9): 334-342.

Al-Asbahi, B.A., Jumali, M.H.H., Yap, C.C., Flaifel, M.H. & Salleh, M.M. 2013a. Photophysical properties and energy transfer mechanism of PFO/Fluorol 7GA hybrid thin films. *Journal of Luminescence* 142: 57-65.

Al-Asbahi, B.A., Jumali, M.H.H., Yap, C.C., Salleh, M.M. & Alsalhi, M.S. 2013b. Inhibition of dark quenching by TiO_2 nanoparticles content in novel PFO/Fluorol 7GA hybrid: A new role to improve OLED performance. *Chemical Physics Letters* 570: 109-112.

Albrecht, C. 2008. Joseph R. Lakowicz: Principles of fluorescence spectroscopy. *Analytical and Bioanalytical Chemistry* 390(5): 1223-1224.

Ciotta, E., Prosposito, P. & Pizzoferrato, R. 2019. Positive curvature in Stern-Volmer plot described by a generalized model for static quenching. *Journal of Luminescence* 206: 518-522.

Cossiello, R.F., Susman, M.D., Aramendía, P.F. & Atvars, T.D.Z. 2010. Study of solvent-conjugated polymer interactions by polarized spectroscopy: MEH–PPV and Poly(9,9′-dioctylfluorene-2,7-diyl). *Journal of Luminescence* 130(3): 415-423.

Hegde, V., Chauhan, N., Kumar, V., Viswanath, C.S.D., Mahato, K.K. & Kamath, S.D. 2019. Effects of high dose gamma irradiation on the optical properties of $Eu3^+$ doped zinc sodium bismuth borate glasses for red LEDs. *Journal of Luminescence* 207: 288-300.

Huang, T.H., Chi, X.C., Xu, T.N., Zhang, J.R., Xu, H.Y., Zhu, Z.Y., Yu, R.B., Wang, Y.H. & Zhang, H.Z. 2018. Effect of Ag nanoparticles on the photoluminescence of poly [2-methoxy-5-(2-ethylhexyloxy)-1,4-phenylene-vinylene]. *Journal of Photochemistry and Photobiology A: Chemistry* 356(2018): 334-339.

Huang, J., Li, G., Wu, E., Xu, Q. & Yang, Y. 2006. Achieving high-efficiency polymer white-light-emitting devices. *Advanced Materials* 18(1): 114-117.

Jumali, M.H.H., Al-Asbahi, B.A., Yap, C.C., Salleh, M.M. & Alsalhi, M.S. 2012. Optoelectronic property enhancement of conjugated polymer in poly (9,9′-di-n-octylfluorenyl-2.7-diyl)/titania nanocomposites. *Thin Solid Films* 524: 257-262.

Karthikeyan, B. 2017. Förster resonance energy transfer and excited state life time reduction of rhodamine 6G with NiO nanorods in PVP films. *Spectrochimica Acta-Part A: Molecular and Biomolecular Spectroscopy* 173: 301-306.

Kasparek, C. & Blom, P.W.M. 2017. Solution-processed multilayer polymer light-emitting diode without intermixing. *Applied Physics Letters* 110(2): 023302.

Lee, S.E., Oh, J.H., Baek, H.J., Kim, S., Do, Y.R. & Kim, Y.K. 2019. Realization of high-color-quality white-by-blue organic light-emitting diodes with yellow and red phosphor films. *Journal of Luminescence* 207: 195-200.

Li, X., Bai, Z., Liu, B., Li, T. & Lu, D. 2017. From starting formation to the saturation content of the β-phase in poly(9,9-dioctylfluorene) toluene solutions. *Journal of Physical Chemistry C* 121(27): 14443-14450.

Liu, J., Shi, Y. & Yang, Y. 2001. Improving the performance of polymer light-emitting diodes using polymer solid solutions. *Applied Physics Letters* 79(5): 578-580.

Madhwal, D., Rait, S.S., Verma, A., Kumar, A., Bhatnagar, P.K., Mathur, P.C. & Onoda, M. 2010. Increased luminance of MEH–PPV and PFO based PLEDs by using salmon DNA as an electron blocking layer. *Journal of Luminescence* 130(2): 331-333.

Nedumpara, R.J., Manu, P.J., Vallabhan, C.P.G., Nampoori, V.P.N. & Radhakrishnan, P. 2008. Energy transfer studies in dye mixtures in different solvent environments. *Optics & Laser Technology* 40(7): 953-957.

Pandey, K.K., Joshi, H.C. & Pant, T.C. 1988. Excitation energy migration and transfer in a dye pair in PMMA. *Journal of Luminescence* 42(4): 197-203.

Perevedentsev, A., Chander, N., Kim, J.S. & Bradley, D.D.C. 2016. Spectroscopic properties of poly(9,9-dioctylfluorene) thin films possessing varied fractions of β-phase chain segments: Enhanced photoluminescence efficiency via conformation structuring. *Journal of Polymer Science, Part B: Polymer Physics* 54(19): 1995-2006.

Prakash, A. & Katiyar, M. 2016. Effect of guest concentration on carrier transportation in blends of conjugated polymers. *Organic Electronics* 39: 50-58.

Schweitzer, C. & Schmidt, R. 2003. Physical mechanisms of generation and deactivation of singlet oxygen. *Chemical Reviews* 103(5): 1685-1758.

Shen, F., He, F., Lu, D., Xie, Z., Xie, W., Ma, Y. & Hu, B. 2006. Bright and colour stable white polymer light-emitting diodes. *Semiconductor Science and Technology* 21(2): L16-L19.

Shin, S.B., Gong, S.C., Lee, H.M., Jang, J.G., Gong, M.S., Ryu, S.O., Lee, J.Y., Chang, Y.C. & Chang, H.J. 2009. Improving light efficiency of white polymer light emitting diodes by introducing the TPBi exciton protection layer. *Thin Solid Films* 517(14): 4143-4146.

Su, H., Wu, F., Shu, C., Tung, Y., Chi, Y. & Lee, G. 2005. Polyfluorene containing diphenylquinoline pendants and their applications in organic light emitting diodes. *Journal of Polymer Science Part A: Polymer Chemistry* 43(4): 859-869.

Thomas, S., Grohens, Y. & Jyotishkumar, P. 2014. *Characterization of Polymer Blends: Miscibility, Morphology and Interfaces*. New York: John Wiley & Sons. pp. 1-901.

Winokur, M.J., Slinker, J. & Huber, D.L. 2003. Structure, photophysics, and the order-disorder transition to the β-phase in poly (9, 9-(di-n, n-octyl) fluorene). *Physical Review B* 67(18): 184106.

Yan, F., Xing, G., Chen, R., Demir, H.V., Sun, H., Sum, T.C. & Sun, X.W. 2015. Efficient three-color white organic light-emitting diodes with a spaced multilayer emitting structure. *Applied Physics Letters* 106(2): 023302.

Yang, S.H. & Zhuang, D.W. 2011. Enhancement of efficiency of multilayer polymer light-emitting diodes by inserting blocking layers. *Journal of Luminescence* 131(4): 801-807.

Zhang, L., Li, X.L., Luo, D., Xiao, P., Xiao, W., Song, Y., Ang, Q. & Liu, B. 2017. Strategies to achieve high-performance white organic light-emitting diodes. *Materials* 10(12): 1378-1434.
Zhou, J., Zou, J., Dai, C., Zhang, Y., Luo, X. & Liu, B. 2018. High-efficiency and high-luminance three-color white organic light-emitting diodes with low efficiency roll-off. *ECS Journal of Solid State Science and Technology* 7(6): R99-R103.

Sameer Albati, Mohammad Hafizuddin Hj. Jumali* & Chi Chin Yap
School of Applied Physics
Faculty of Science and Technology
Universiti Kebangsaan Malaysia
43600 UKM Bangi, Selangor Darul Ehsan
Malaysia

Bandar Ali Al-Asbahi & Saif M.H. Qaid
Department of Physics and Astronomy
College of Science, King Saud University
Riyadh 11451
Saudi Arabia

Bandar Ali Al-Asbahi
Department of Physics, Faculty of Science
Sana'a University
Yemen

*Corresponding author; email: hafizhj@ukm.edu.my

Received: 16 December 2019
Accepted: 22 May 2020